Lattice dynamics and effects of anharmonicity in different phases of caesium hydrogen sulphate

1994 J. Phys.: Condens. Matter 6 5823

(http://iopscience.iop.org/0953-8984/6/30/005)

J. Phys.: Condens. Matter 6 (1994) 5823–5832. Printed in the UK

Lattice dynamics and effects of anharmonicity in different phases of caesium hydrogen sulphate

A V Belushkin†‖, M A Adams†, A I Kolesnikov‡¶ and L A Shuvalov§

† Rutherford Appleton Laboratory, Chilton, Didcot, Oxon OX11 0QX, UK

‡ Institut für Festkörperforschung, Forschungszentrum Jülich, Jülich D-52425, Germany

§ Institute of Crystallography, 117333 Moscow, Russian Federation

Received 6 April 1994

Abstract. The inelastic neutron scattering spectra of caesium hydrogen sulphate ($CsHSO_4$) in three different low-temperature crystallographic phases have been obtained. One of the phases was obtained by applying a pressure of 1.7 GPa at ambient temperature.

A comparative analysis of the vibrational spectra is presented. It is shown that the proton dynamics in the hydrogen bonds of the two ambient pressure phases are almost totally decoupled from the dynamics of the other atoms.

Anharmonicity plays an important role in the dynamical properties of the ambient pressure phases. It is observed that the effects of anharmonicity in one of the ambient pressure phases can be explained within the framework of the simple anharmonic oscillator model. For the other ambient pressure phase the model of bound two-phonon (biphonon) states is required to explain the data. On the other hand in the high-pressure crystalline phase the proton dynamics exhibit an almost purely harmonic behaviour coupled with a strong interaction between the hydrogen-bond bending modes and SO_4^{2-} ion internal vibrations.

1. Introduction

$CsHSO_4$ exists in a variety of phases depending upon the temperature and pressure [1–3]. At ambient pressure the structural and dynamical properties of the different phases have been extensively investigated by different methods [1, 3, 4] but little is known about the properties of the high-pressure phases. Optical spectroscopy studies have left some uncertainties regarding band assignment, and previous neutron spectroscopy results obtained at ambient pressure suffered from poor resolution [4]. Because of the rich variety of phase transitions, the metastable character of some phases [4, 5] and the large amplitudes of vibration of the hydrogen atoms, it is natural to expect the presence of strong anharmonic effects in the dynamics and especially the proton dynamics.

In this paper we present a high-resolution inelastic neutron scattering study of the dynamics of three low-temperature phases of $CsHSO_4$. The investigations were undertaken to establish the correct assignment of the vibrational modes, to compare the dynamical properties of different crystal phases and to study the effects of anharmonicity on some vibrational modes. We shall use the notation of phases according to [2, 4].

In section 2 some structural features of the crystalline phases studied are discussed. Section 3 is devoted to the experimental details. Results of the high-resolution neutron scattering experiments are discussed in section 4 and basic results are collated in section 5.

‖ On leave from: Frank Laboratory of Neutron Physics, JINR, 141980 Dubna, Russian Federation.

¶ On leave from: Institute of Solid State Physics, 142342 Chernogolovka, Russian Federation.

0953-8984/94/305823+10$19.50

2. Crystal structures

2.1. Phase III

$CsHSO_4$ grown from aqueous solution crystallizes into phase III. The atomic structure of this phase has been determined by several authors [6–8]. It is monoclinic, with space group $P2_1/c$, with four structural units in the unit cell. The sulphate ions are linked by hydrogen bonds to form zig-zag chains along the b crystal axis.

At room temperature, the unit cell parameters are: $a = 8.214$ Å, $b = 5.809$ Å, $c = 10.984$ Å, $\beta = 119.39°$, $V = 456.7$ Å^3. The hydrogen bond length (O–O distance) is 2.555 Å [7]. A view of the crystal structure of phase III projected along the crystal a axis is shown in figure 1(a). No phase transitions have been observed when this phase is cooled down to liquid helium temperatures [4, 6]. Phase III is unique for $CsHSO_4$ and has no analogue among the other $MeHAO_4$ structures (see [7] and references therein). This phase is metastable [5, 7] and this is discussed in the next section.

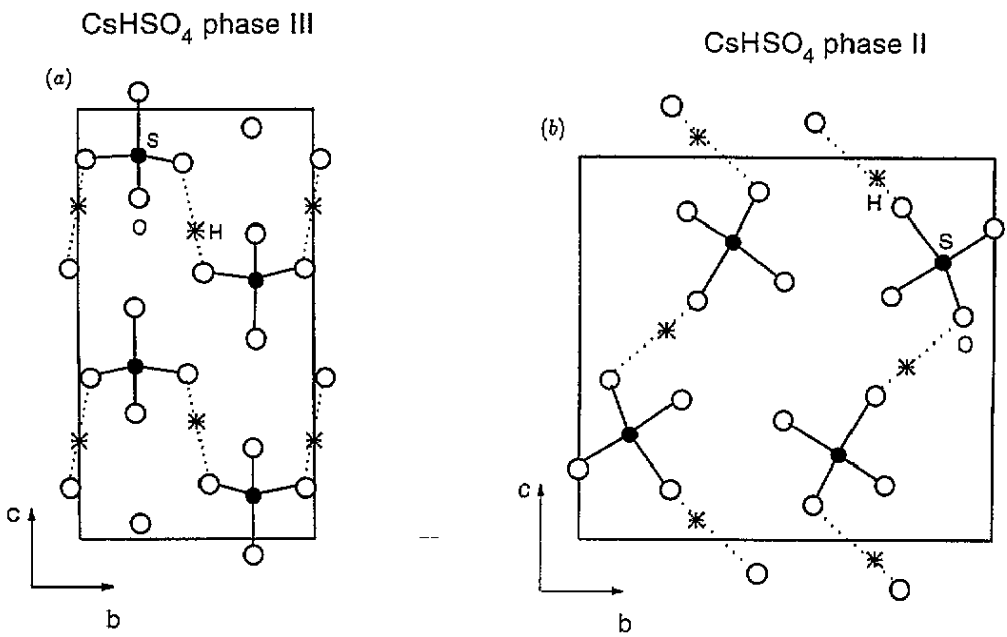

Figure 1. The structure of the phase III of $CsHSO_4$ as projected along the a crystal axis (a) and the same projection for the phase II (b). The Cs atoms are not shown for clarity.

2.2. Phase II

When heated, phase III transforms into phase II at 349 K (this temperature is well defined for the single crystal [8]; on polycrystalline samples a broad temperature range from 330 to 370 K corresponds to the coexistence of phases III and II [4]). After the III–II transition, cooling of the sample all the way down to liquid helium temperature does not lead to a transition back into phase III [4, 6, 8]. Special conditions are required to restore phase III after the III–II phase transition [5, 9]. The structure of phase II is monoclinic, space group $P2_1/c$, with four structural units in the unit cell. The room temperature unit cell parameters

are: $a = 7.763$ Å, $b = 8.127$ Å, $c = 7.705$ Å, $\beta = 110.80°$, $V = 454.4$ Å^3 [8]. In this phase the sulphate ions are again linked by hydrogen bonds into zig-zag chains but these now go along the c crystal axis. The hydrogen bond length is 2.624 Å [8] which within experimental error coincides with the deuterium bond length in $CsDSO_4$ (phase II) obtained by x-ray (2.626 Å, [10]) and neutron diffraction (2.633 Å, [11]) techniques. The projection along the a crystal axis of the structure of phase II is shown in figure 1(b).

2.3. Phase V

The application of high pressure results in a number of new phase transitions [2]. At room temperature and above 1.4 GPa, phase V is realized. The transtion into this phase is accompanied by a substantial decrease in the unit cell volume. The crystal structure of this phase is not known. Because there are no studies of the P–T phase diagram below room temperature we shall refer below to the inelastic neutron scattering data obtained at a temperature 30 K and pressure of 1.7 GPa as corresponding to phase V of $CsHSO_4$.

3. Experiment

The sample in phase III was obtained by slow evaporation of an aqueous solution of caesium carbonate and sulphuric acid. To prepare phase II the sample was heated to 100 °C for several hours, then cooled to room temperature and placed in an air-tight container before the measurements. The structure of the phases was checked by neutron diffraction. The sample in phase V was obtained from the phase III sample by applying a high pressure. The sample was mixed with a pressure-transmitting fluid (Fluorinert FC-75) to ensure hydrostaticity and inserted into a clamped high-pressure cell of the McWhan design which had been modified to include collimation and shielding components in order to improve the signal–background ratio [12]. Using a hydraulic press, a load corresponding to a sample pressure of 1.7 ± 0.1 GPa (determined from calibration experiments) was applied at room temperature.

The inelastic neutron scattering (INS) experiments were performed on the TFXA spectrometer at the spallation neutron source, ISIS, Rutherford Appleton Laboratory, UK [13]. The spectra were normalized to the monitor counts and converted from the neutron time-of-flight scale into the scattering law $S(Q, \omega)$ using standard programs [13]. The ambient pressure measurements were made with the samples being placed in Al foil sachets and then loaded into a cryostat on the neutron beamline. The measurements were performed at a temperature of 30 K. For the high-pressure measurement the pressure cell was pre-cooled using liquid nitrogen and then inserted into the cryostat. The neutron scattering measurement began when the cell temperature was below 50 K. A separate measurement with an empty pressure cell was made for background subtraction purposes. In order to make a comparative analysis, the spectra for all three phases were normalized to equal integrated intensity in the energy region from 2–250 meV. The lower bound is defined by the spectrometer resolution and the upper bound corresponds to the maximum energy above which no sharp features were observed in the neutron spectra.

4. Results and discussion

4.1. Inelastic neutron scattering spectra

The INS spectra of phases III, II and V of CHS are shown in figures 2, 3 and 4 respectively as solid lines. Band assignment is also presented in the figures. The spectra from phases

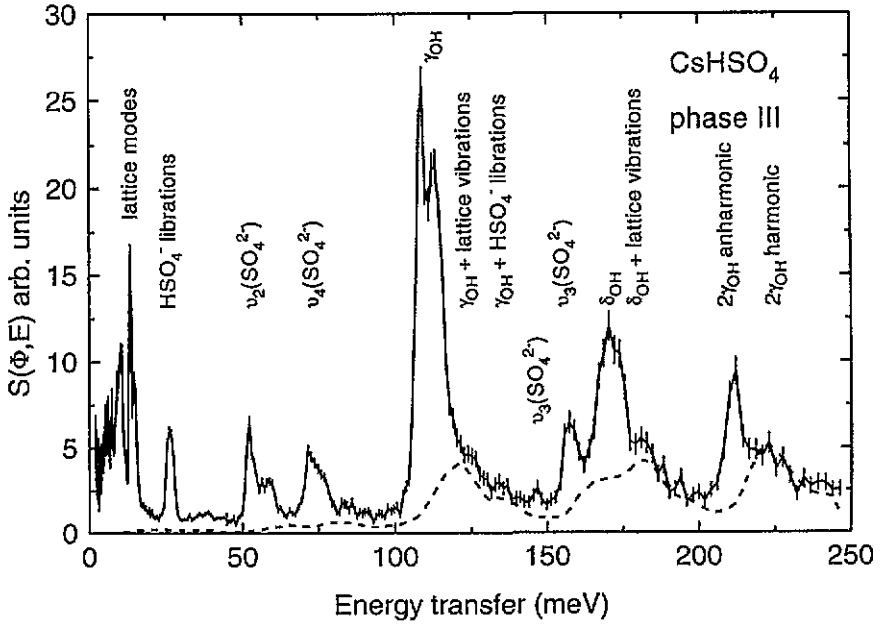

Figure 2. The inelastic neutron scattering (INS) spectrum from phase III of $CsHSO_4$. The solid line with error bars shows experimental data and the broken line corresponds to the estimated multiphonon contribution (see the text).

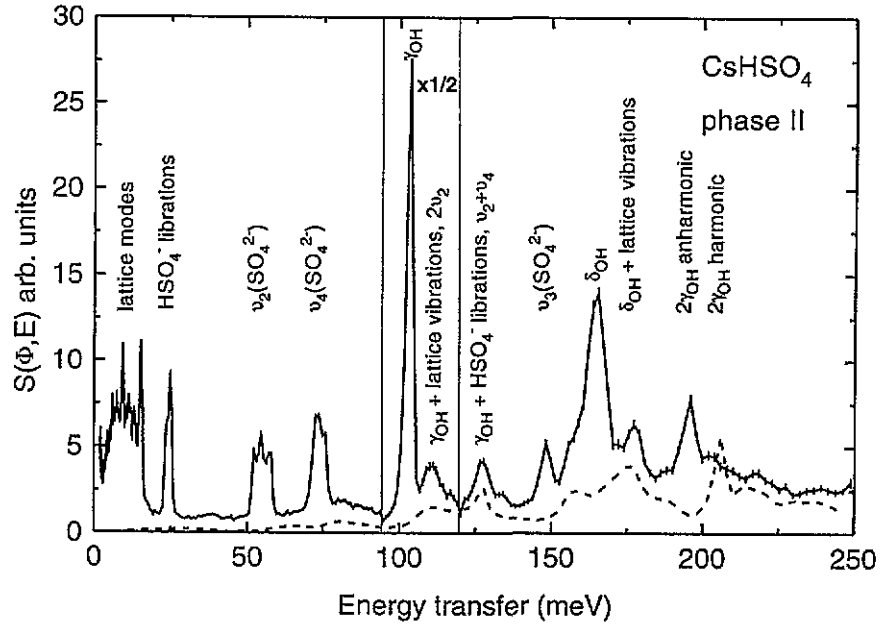

Figure 3. The INS spectrum from phase II. The definitions are the same as in figure 2.

III and II are similar to those obtained earlier [4] but the much better resolution of the present experiment makes it possible to observe fine spectral details. One can separate

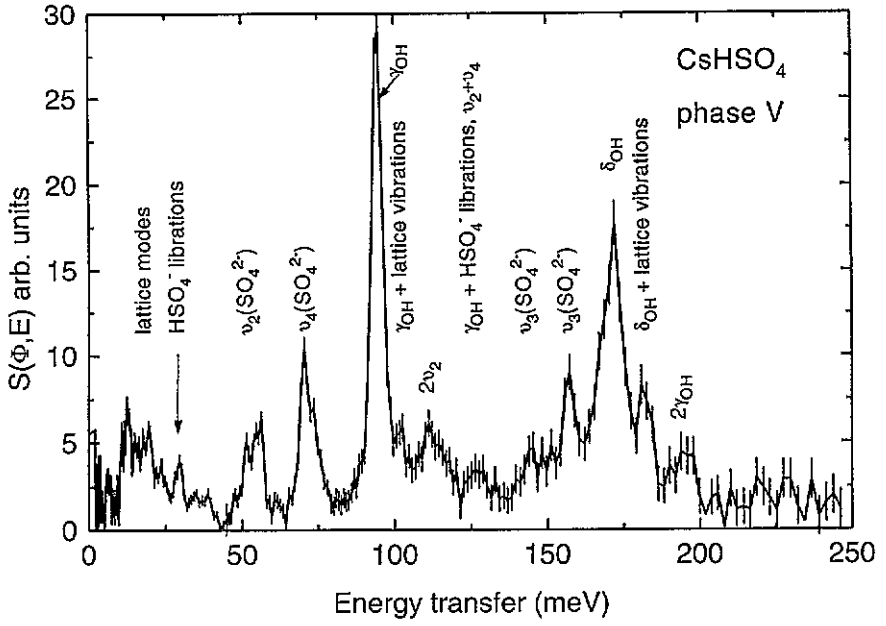

Figure 4. The INS spectrum from phase V.

out several specific regions in all the spectra. Below 45 meV, lattice vibrations and HSO_4^- librational modes are responsible for spectral intensities. The region between 45 and 80 meV corresponds to the internal deformational modes, ν_2 and ν_4, of the SO_4^{2-} anion. In the energy interval from 80 to 120 meV the out-of-plane hydrogen-bond bending mode, γ_{OH}, produces intense spectral features. The SO_4^{2-} stretching vibrations, ν_1 and ν_3, and in-plane hydrogen-bond bending mode δ_{OH}, occur between 120 and 180 meV. The hydrogen-bond symmetric stretching vibrations have frequencies in the region 290–350 meV [14] but were not reliably observed in our neutron spectra and therefore will not be discussed.

4.1.1. Lattice vibrations and HSO_4^- librations. Because the samples were polycrystalline a detailed analysis of the lattice vibrations is not possible. However, some qualitative conclusions can be reached. For phases III and II (figures 2 and 3) the upper energy boundaries for the lattice modes have the same value of approximately 16 meV. Some sharp and rather intense features can be observed in this region and these indicate the involvement of protons in these vibrational modes. The existence of sharp lines is also an indication of weak coupling of these modes with other types of vibrations. In contrast, for phase V, the upper boundary for the lattice vibrations spreads up to 45 meV and sharp features disappear indicating an increase in the strength of the interaction between different vibrational modes as a result of the application of pressure. This conclusion will be further supported in the later discussion.

The HSO_4^- librational mode in phase III is centred at 26.6 meV and in phase II at 25.0 meV. At first sight this fact is surprising because the unit cell volume of phase II is smaller than that of phase III (see sections 2.1 and 2.2). However the higher frequency of the librational mode in phase III correlates well with the smaller distance between HSO_4^- goups in this phase in comparison with phase II (see figure 1). As one would expect, the application of pressure should normally lead to an increase in librational-mode vibrational frequencies. This expectation is confirmed by the higher librational frequency of the HSO_4^-

ion in phase V (30 meV) in comparison with the ambient pressure phases. In this case the increase in librational frequency correlates well with the decrease of the unit cell volume accompanying the transition into phase V [2]. One should bear in mind, however, that in this phase the librational mode probably has a mixed character because it falls into the lattice mode region and therefore strong mixing between different types of vibrations is likely.

The integrated spectral intensity in this region remains constant for all the phases within experimental error. This fact indicates that the coupling of these vibrational modes with higher-energy vibrations is always weak.

4.1.2. Internal vibrations of the SO_4^{2-} anion. The assignment of these modes is rather straightforward based upon the known frequencies for the free sulphate ion and the published single-crystal Raman spectroscopy data [14]. The free sulphate anion has one A_1-type vibration with frequency $\nu_1 = 121.9$ meV, one of type E with $\nu_2 = 55.8$ meV, and two of type F_2 with $\nu_3 = 137.0$ meV and $\nu_4 = 75.8$ meV. Because of the crystalline electric field the degeneracy of these vibrations is lifted which increases the number of lines corresponding to each type of tetrahedron vibration. In the region between 50 and 65 meV three lines are resolved in our experiment which can be attributed to the ν_2 vibrational mode. Similarly for the region containing the ν_4 mode two lines are observed in all phases. A fit of these lines with Gaussians (which is a good approximation of the intrinsic line shape convoluted with the instrument resolution) for each of the phases gives the results in table 1. The line width is larger for phases III and V in comparison with phase II in which the line width only slightly exceeds the spectrometer resolution. This is an indication that the interaction between modes in phase II is weak and therefore they are practically dispersionless whereas in phases III and V there is a pronounced interaction between the modes leading to dispersion. The difference between phases III and II is to be expected when comparing the two structures (figure 1). The distance between nearest-neighbour sulphate anions is smaller in phase III than in phase II and this tends to increase the effect of correlation between the vibrational modes. As mentioned above, pressure decreases the unit cell volume and therefore in phase V we again expect stronger mode mixing resulting in the observed line broadening.

Table 1. Vibrational energies of the SO_4^{2-} ion

	Vibrational energy (meV) in each phase		
Vibrational mode	III	II	V
ν_2	52.3, 53.8, 59.1	52.7, 54.8, 57.6	51.8, 54.5, 56.7
ν_4	72.7, 77.0	73.1, 75.8	70.8, 74.6
ν_3	149.0, 159.6	149.0, 158.5	145.0, 157.6

The integrated intensity of the deformational modes, ν_2 and ν_4, remains the same in phases III and II but increases in phase V. This indicates a stronger interaction of these modes in phase V with higher-energy vibrations, namely hydrogen-bond bending modes.

Finally we note that the centre of gravity for the ν_2 and ν_4 vibrations has the highest value in phase III and the lowest in phase V. Therefore the decrease in the unit cell volume leads to a decrease in frequency of the deformational modes of the sulphate anion in caesium hydrogen sulphate. This effect has been previously observed [14] for phases III and II.

The assignment of the ν_3 mode is based upon the Raman data [14]. As one can see from the values shown in table 1 there is the same trend for this stretching mode as that

observed for the deformational vibrations, namely the frequency decreasing with decreasing unit cell volume.

The ν_1 mode was not reliably observed in our spectra because of its low intensity and coincidence of its frequency with the hydrogen-bond bending modes which have the strongest intensity in the neutron spectra.

4.1.3. Hydrogen-bond vibrations. Three types of proton motion are possible in the hydrogen bond. They are the out-of-plane bending mode, γ_{OH}, the in-plane bending mode, δ_{OH}, and the symmetric and asymmetric stretching modes, ν_s and ν_{as}. The stretching modes were not reliably observed in our neutron spectra and will not be discussed.

The γ_{OH} mode in phase III is split into two (doubly degenerate) lines with frequencies 109.3 and 114.2 meV. The single (quadruply degenerate) line corresponding to this mode in phase II has frequency 103.7 meV. As expected the integrated intensity of this single line is equal to the integrated intensity of the two observed lines in phase III (note the scaling factor for this mode in figure 3). The splitting of the out-of-plane mode in phase III is attributable to proton–proton dynamical correlations. From figure 1 it can be seen that in phase II the distance between nearest-neighbour protons along the *b*-axis is larger than in phase III and therefore the proton–proton correlations in the former are absent. In phase V a single line is also observed and therefore, in analogy with phase II, we assume that the distance between nearest-neighbour protons in the unit cell of phase V should be larger than that in phase III. The intensity of the γ_{OH} mode in phase V is lower than that in phases III and II. We noted above an increase in intensity of the deformational modes of the SO_4^{2-} tetrahedron in phase V in comparison with phases III and II. A calculation of the integrated intensity of the SO_4^{2-} deformation modes plus the intensity of the γ_{OH} mode have shown that in all phases it remains constant within experimental error. Therefore we conclude that in phase V there is a strong mixing between internal deformational modes of the sulphate anion and the γ_{OH} hydrogen-bond bending mode.

There is an empirical relationship [15, 16] between the frequency of the γ_{OH} mode and R_{OO}, the distance between the two oxygens involved in the hydrogen bond. The corresponding formula is $R_{OO} = 3.01$ Å-4.4×10^{-4} Å/cm$^{-1} \times \nu(\gamma_{OH})$, where the frequency is given in cm^{-1} (1 meV = 8.066 cm^{-1}). This relationship works very well in phase II but not in phase III. The absence of a simple relationship between the observed frequencies and R_{OO} distances has also been observed for other hydrogen-bonded systems in which strong proton–proton dynamical correlations play an important role [17]. Therefore, we believe that these correlations are similarly responsible for the violation of the empirical relation in phase II of $CsHSO_4$. In phase V no splitting of the γ_{OH} mode is observed and so it is expected that the above mentioned relationship should work in this phase. From the observed frequency of the γ_{OH} mode in this phase the estimated distance R_{OO} is 2.67 Å.

The in-plane δ_{OH} mode produces a single spectral line in all phases. For phase III it would be expected that this mode should be split due to the proton–proton correlations, similar to that observed for the γ_{OH} mode. However, it may be that the splitting is beyond the present resolution limits of the spectrometer used. In phase III the frequency of the δ_{OH} mode is 171.8 meV, in phase II 165.9 meV and in phase V 172.0 meV. No simple relations between the frequency of this mode and any other vibrational frequencies or structural properties of the system have been found so far. Therefore we shall not discuss this type of vibration any further.

4.2. Multiphonon processes

As one can see from figures 2–4 some spectral features are left unassigned. To understand their nature we performed calculations of multiphon scattering processes using the program

described in [18]. This program uses an iterative procedure to evaluate the multiphonon contribution from the experimental data. However, this program can only work satisfactorily if there is a well defined region in the neutron spectrum which corresponds to particular atomic or molecular unit vibrations. Then spectrum normalization can be done correctly and the calculations give consistent results. In our case this condition is approximately valid only for phases III and II where the out-of-plane bending mode is well defined in the spectra and its interaction with other vibrations is small. In phase V, because of the strong mixing of this mode with the vibrations of the sulphate ion tetrahedron, the situation becomes more complicated. The other problem in calculations for the phase V spectra is due to the poorly defined low-energy part of the spectrum (below 10 meV). This is caused by a large background from the high-pressure cell in this energy region.

Indeed calculations gave a reasonable result for the phases III and II but for phase V an agreement between calculated and observed multiphonon profiles could not be reached. In figures 2 and 3 the calculated multiphonon profiles using the harmonic approximation are shown by the dashed lines. The assignment of the corresponding multiphonon features is presented in the figures. For phase V this assignment is made on the basis of a comparative analysis with phases III and II. The interesting observation is that while most of the multiphonon features are well reproduced by the calculation (at least qualitatively) there are lines in the spectra of phases III and II above 190 meV which are not explained by the essentially harmonic calculations. We shall discuss these features in more details below.

4.2.1. Phase V. As mentioned above, a direct calculation of the multiphonon contribution to the neutron spectrum of this phase was not successful. However, the assignment of the multiphonon features is rather straightforward for this phase on the basis of: (a) the expected positions for the overtones, combinations and phonon wings within the harmonic approximation; and (b) a comparison with the results of calculations for phases III and II. Between 100 and 140 meV the spectral features are due to combinations of the γ_{OH} fundamental mode with the lattice and HSO_4^- librational modes and overtones and combinations of the ν_2 and ν_4 modes. The peak at 183 meV is assigned to be the combination of the δ_{OH} bending mode and the lattice modes. The peak at 195 meV is assigned to be mainly due to the first overtone of the γ_{OH} mode. No other lines are left unassigned in the spectrum. The frequencies of all the multiphonon wings expected in the harmonic approximation. Therefore one can conclude that phase V shows a reasonably harmonic behaviour.

4.2.2. Phase II. In this phase the calculation in the energy region above 185 meV predicts an almost perfect profile of the first γ_{OH} overtone and the associated phonon wings but the experimental features are shifted to lower frequencies. This shift is due to anharmonic effects. The vibrations of the proton in the hydrogen bond for this phase are decoupled from the dynamics of other atoms as discussed above. Therefore in calculating the anharmonic energy level scheme one can consider the proton in this phase to be a single-particle oscillator. Then, the energy levels are given by [19]:

$$E_n = hc[v(n+\tfrac{1}{2}) - xv(n+\tfrac{1}{2})^2 \ldots] \tag{1}$$

where $n = 0, 1, 2, \ldots$ is the number of energy level and x is the anharmonicity parameter. Taking into consideration only the first anharmonic term one gets from the ratio of energies of the $(0 \rightarrow 1)$ and $(0 \rightarrow 2)$ transitions:

$$x = \frac{2\Delta E(0 \rightarrow 1) - \Delta E(0 \rightarrow 2)}{6\Delta E(0 \rightarrow 1) - 2\Delta E(0 \rightarrow 2)}. \tag{2}$$

Using (2) and the experimentally observed $\Delta E(0 \rightarrow 1) = 103.7$ meV and $\Delta E(0 \rightarrow 2) = 196.6$ meV, the anharmonicity parameter for the hydrogen-bond bending mode in phase II is calculated to be 0.0472.

4.2.3. Phase III. In this phase, calculations of the multiphonon contribution to the neutron spectrum gave a very good description of all extra features unassigned to the fundamental vibrations, except for an extra sharp line at 213.1 meV. This line cannot be considered to be due to a simple anharmonic shift of the first overtone of the γ_{OH} mode. The intensity of this line is even higher than the intensity of the γ_{OH} overtone in phase II. In phase II all the intensity of the fundamental which produces the overtone is concentrated in a sharp single line. In contrast, in phase III the fundamental is split into two lines. Thus one should expect that in the latter case the overtone will be not as sharp as in phase II but rather a broad feature. Indeed the corresponding sharp harmonic feature does not appear in the calculations. It would therefore be very artificial to assume that the sharp feature observed in phase III is due to a simple anharmonic shift of the corresponding harmonic overtone as in phase II. We believe that this feature is due to the creation of a bound two-phonon state (biphonon). The theory of such many-phonon bound states (see [20] and references therein) predicts that for strong anharmonic phonon–phonon interactions sharp and rather intense resonance peaks can appear in the spectra close to the continuum of the unbound multiphonon bands. It was also shown [21] that the formation of the bound multiphonon states is more likely for crystals with low dimensionality. The existence of quasi-one-dimensional hydrogen-bond chains and strong proton–proton correlations in phase III favours the appearance of such bound states. The bound two-phonon peak appears at an energy below the low-frequency edge of the unbound multiphonon band and its width is approximately twice as large as the width of any one of the doubly degenerate lines of the split γ_{OH} fundamental mode. This observation agrees with the predictions of the simplest phenomenological approach to bound multiphonon states [20].

5. Conclusions

(i) Because of the high sensitivity of neutron scattering to the vibrations of protons the assignment of HSO_4^- librations and hydrogen-bond vibrations is unique and gives additional and more precise information than the optical spectroscopy studies.

(ii) The analysis of the spectra has shown that in the metastable phase III there is a strong proton–proton dynamical correlation effect. This leads to the splitting of the hydrogen-bond bending vibrations and to the violation of the simple empirical relation between the frequency of the out-of-plane hydrogen-bond-bending mode and the R_{OO} distance between the oxygens involved in the hydrogen bond. Together with similar observations in other systems [17] it can be concluded that these proton–proton correlations are a major reason for the simple empirical rule being not universally valid. The sharp spectral feature observed in the multiphonon energy region at 213.1 meV cannot be explained within the framework of the simple anharmonic oscillator model. However, it can be reasonably ascribed to a bound two-phonon state. The strong proton–proton correlations along the *b* crystal axis in phase III are responsible for the appearance of such biphonon states.

(iii) In phase II the proton dynamics is strongly decoupled from the lattice. It can be described within the framework of the anharmonic oscillator model. From the experimentally observed frequency shift of the first overtone of the out-of-plane hydrogen-bond bending mode the anharmonicity constant is calculated to be 0.0472.

(iv) The application of high pressure, as is usually to be expected, leads to more harmonic behaviour in phase V. In this phase a strong interaction of the hydrogen-bond modes with the internal modes of the sulphate anion is observed. The application of pressure also leads to an increase in the cut-off frequency of the lattice vibrations and the frequency of HSO_4^- librations. On the other hand, the frequency of the out-of-plane hydrogen-bond-bending mode decreases in comparison with the corresponding values observed for phases III and II realized at ambient pressure. This observation allows us to assume that the hydrogen-bond length (distance R_{OO}) increases as a result of pressure. The estimated value for this distance is 2.67 Å. It would be interesting to see what value a neutron diffraction experiment provides.

Acknowledgments

The authors thank the Rutherford Appleton Laboratory for the access to the ISIS facilities. One of us (AIK) thanks the Alexander von Humboldt Foundation for financial support.

References

[1] Komukae M, Osaka T, Makita Y, Ozaki T, Itoh K and Nakamura E 1981 *J. Phys. Soc. Japan* **50** 3187
[2] Ponyatovskii E G, Rashchupkin V I, Sinitsyn V V, Baranov A I, Shuvalov L A and Shchagina N M 1985 *JETP Lett.* **41** 139
[3] Friesel M, Baranowski B and Lundén A 1989 *Solid State Ion.* **35** 85
[4] Belushkin A V, Natkaniec I, Plakida N M, Shuvalov L A and Wasicki J 1987 *J. Phys. C: Solid State Phys.* **20** 671
[5] Lundén A, Baranowski B and Friesel M 1994 *Proc. Int. Seminar on Superprotonic Conductors (Dubna, Russia, 1993); Ferroelectrics* at press
[6] Balagurov A M, Belushkin A V, Beskrovnyj A I, Vratislav S, Wasicki J, Dutt I D, Dlouha M, Jirak Z, Natkaniec I, Savenko B N and Shuvalov L A 1985 *JINR Rapid Commun.* **13-85** 18
[7] Itoh K, Ukeda T, Ozaki T and Nakamura E 1990 *Acta. Crystallogr.* C **46** 358
[8] Lipkowski J, Baranowski B and Lundén A 1993 *Polish J. Chem.* **67** 1867
[9] Baranowski B, Friesel M and Lundén A 1987 *Z. Naturf.* a **42** 565
[10] Merinov B V, Baranov A I, Shuvalov L A and Maksimov B A 1986 *Sov. Phys.–Crystallogr.* **31** 264
[11] Belushkin A V, David W I F, Ibberson R M and Shuvalov L A 1991 *Acta Crystallogr.* B **47** 161
[12] Adams M A and Tomkinson J 1992 *Physica* B **180 & 181** 694
[13] Penfold J and Tomkinson J 1986 *Rutherford Appleton Laboratory Report* RAL-86-019
[14] Dmitriev V P, Loshkarev V V, Rabkin L M, Shuvalov L A and Yuzyuk Yu I 1986 *Sov. Phys.–Crystallogr.* **31** 673
[15] Novak A 1974 *Struct. Bonding* B **18** 177
[16] Howard J, Tomkinson J, Eckert J, Goldstone J A and Taylor A D 1983 *J. Chem. Phys.* **78** 3150
[17] Fillaux F and Tomkinson J 1992 *J. Mol. Struct.* **270** 339
[18] Kolesnikov A I, Prager M, Tomkinson J, Bashkin I O, Malyshev V Yu and Ponyatovskii E G 1991 *J. Phys.: Condens. Matter* **3** 5927
[19] Colthup N B, Daly L H and Wiberley S E 1990 *Introduction to infrared and Raman Spectroscopy* 3rd edn (San Diego, CA: Academic)
[20] Agranovich V M 1983 *Spectroscopy and Excitation Dynamics of Condensed Molecular Systems* ed V M Agranovich and R M Hochstrasser (Amsterdam: North-Holland) p 83
[21] Agranovich V M, Dubovski O A and Orlov A V 1986 *Phys. Lett.* **119** 83; 1989 *Solid State Commun.* **70** 675